Progress In Electromagnetics Research Letters, Vol. 123, 95-103, 2025

PIER Letters

(Received 7 October 2024, Accepted 4 November 2024, Scheduled 3 December 2024)

Optimize the Performance of Reconfigurable Antenna Based on Laser Treatment for Sub-6 GHz Applications

Qasim H. Kareem[1,*], Laith W. Abdullah[2], Rana A. Shihab[3], Firas A. J. Al-Hasani[1], and Suhail N. Abdullah[1]

[1]*Electrical Engineering Department, Al-Iraqia University, Baghdad, Iraq*
[2]*Communication Techniques Engineering Department, Al-Furat Al-Awsat Technical University, Najaf, Iraq*
[3]*QA & Accreditation Department, University of Baghdad, Baghdad, Iraq*

ABSTRACT: The development of adaptable and efficient antenna designs has been required due to the growing demand for high-performance wireless communication systems driven by the increasing availability of online video streaming and multimedia devices. The design and implementation of a compact, reconfigurable C-shaped patch antenna that is specifically designed for 5G applications in the sub-6 GHz spectrum is presented in this paper. The antenna, which measures $20 \times 30\,\text{mm}^2$, can operate at five resonance frequencies within the 4 to 6 GHz range. Laser treatment is applied to optimize bandwidth and gain. Following the treatment, the antenna attained a bandwidth of 1100 MHz and an improved gain of 5.2 dBi at 5 GHz, as opposed to its initial gain of 4.3 dBi. The system functioned effectively since the reflection coefficient was less than -10 dB over the desired frequency ranges. The design's stable performance, compact integration, and varactor diode frequency adjustment make it desirable for wireless applications. Results exhibited a considerable match between simulated and measured data, demonstrating the promise of this reconfigurable antenna for next-generation wireless communication systems.

1. INTRODUCTION

The field of wideband antennas with high gain is experiencing significant growth, especially in the domains of medical imaging, radar, and defensive communication. Planar microstrip antennas are commonly employed for their benefits, including cost-effectiveness, compact footprint, and seamless interaction with other components [1–3].

Nevertheless, despite these numerous benefits, microstrip antennas have several disadvantages, including limited efficiency and narrow bandwidth. Previous studies [4–10] indicate that co-planar antennas [4] enhance bandwidth by optimizing the dispersion of electromagnetic fields. Modifications to the notch gap [5] improve bandwidth and directivity. Slotted patch antennas [6] improve bandwidth by incorporating resonant slots that change current paths. Defected ground structures (DGSs) [7] are known for attenuating surface waves and enhancing impedance bandwidth. Incorporating parasitic elements into co-planar [8] or stacked designs [9, 10] enhances the effective aperture and streamlines multi-band operations. The dimensions and bandwidth of the microstrip antenna are closely correlated with the substrate's dielectric constant. The substrate's high dielectric constant results in a reduced antenna size, while the substrate's low dielectric constant produces a larger bandwidth [11–13]. The dimensions of the antenna and bandwidth are in a trade-off relationship. However, parametric analysis is the predominant method employed in the current literature to optimize antenna parameters.

The rapid development of various services has caused congestion inside the frequency band, leading to elevated spectrum licensing expenses and increasing customer per-bit rates. To solve these problems, frequency reconfigurable antenna systems are a good idea. They make it possible to send large amounts of data quickly while making good use of spectrum resources for many different wireless protocols [14, 15]. These antennas at the front ends of cognitive systems enable smooth and interference-free radiation by allowing seamless transitions across different bands.

The main objective of this work is to develop and manufacture antennas capable of adjusting both frequency and radiation patterns based on integrating a varactor diode as the tuning mechanism. Existing literature has identified several reconfigurable antennas operating within the 1.8–4.5 GHz range [16–25]. Ref. [16] presents a broad-band right hand circular polarization (RHCP)/left hand circular polarization (LHCP) patch antenna array with an E-shaped element. Particle Swarm Optimization achieved 17% axial ratio (AR) bandwidth. Measuring the isolated element with micro-electromechanical switches (MEMSs) on a 0.092 substrate validated this achievement. Rotated elements are used for pattern symmetry. The suggested antenna in [17] uses a microstrip feed and a circular radiating element. For reconfigurability, the circular radiating element has three patches and silicon PIN diodes as switches. In each of the three patches, slots of various shapes cover 2.4, 3.6, 4.9, 5.1, and 5.9 GHz with an antenna size of $47 \times 35\,\text{mm}^2$. Ref. [18] illustrates a reconfigurable antenna with two quarter-wavelength radial radiators at the top layer. Four PIN diodes control the ra-

* Corresponding author: Qasim Hadi Kareem (qasim.hadi2017@gmail.com).

doi:10.2528/PIERL24100702

Published by THE ELECTROMAGNETIC ACADEMY

diation direction. The antenna has a bandwidth (BW) of 1.88–2.64 GHz (34% fractional BW) and a peak gain of 3.7 dBi.

A three-beam-guiding radio frequency (RF) MEMS-based pattern reconfigurable antenna is presented in [19]. The L-band restricts the antenna's pattern reconfiguration capability, which has a resonance frequency of 1.8 GHz. The RF MEMSs operate in three modes: on, off, and peak gain, with a patch area of $37 \times 67.5\,\text{mm}^2$. The respective values are 6.25 dBi, 6.28 dBi, and 4.01 dBi. A compact reconfigurable monopole antenna in [20] initially functions across a wide frequency range of 4.0–7.8 GHz. By integrating two pin diodes and adjusting their switching states, the antenna can be reconfigured to operate in single-band (3.3–4.2 GHz) and dual-band (3.3–4.2 GHz and 5.8–7.2 GHz) modes with its compact size of $25 \times 15\,\text{mm}^2$ at 3.3 GHz. Ref. [21] presents a reconfigurable antenna in polarization controlled by an open stub branch-line coupler feed network. The antenna, occupying a $150 \times 150\,\text{mm}^2$ area, achieves a tunable impedance bandwidth of 2.0 GHz to 3.0 GHz (40%) by varying the capacitance of four varactor diodes positioned between the circular patch and ring. The impedance bandwidth of the feed network ranges from 1.5 GHz to 3.5 GHz [22]. The article describes a circular patch antenna with frequency-changing capabilities featuring a rectangle and narrow slots. Like a dipole, the antenna produces consistent radiation patterns. Under consideration, its frequency can continually vary between 1.91 and 2.77 GHz. The antenna frequency is controlled by a DC biasing network with three RF varactor diodes on the narrow slot-DGS. The total size of the antenna, including the biased circuit, is $50.5 \times 41.5\,\text{mm}^2$.

A frequency-tunable antenna with dimensions of $31 \times 42\,\text{mm}^2$ that is accomplished by toggling two PIN diodes is illustrated in [23]. The structure demonstrates a multi-band response with four bands, providing a tunability of 700 MHz and a minimum return loss of -28 dB. Ref. [24] introduces a patch antenna that can be reconfigured to accommodate applications in the S and C bands of the RF spectrum. The antenna can be reconfigured to operate at three primary frequencies: 2.07 GHz, 4.63 GHz, and 6.22 GHz, with a switching voltage of less than 0.9 V, by utilizing a single PIN diode on the ground plane. The antenna is designed on an FR-4 substrate with dimensions of $70 \times 60\,\text{mm}^2$ and is characterized by a rectangular ring-shaped radiating patch. Ref. [25] presents a compact wide-band tuning-reconfigurable antenna designed explicitly for sub-6 GHz applications. A matching stub and a C-shaped monopole element can be employed to adjust the frequency across two resonant bands, 4 to 5.18 GHz and 5.45 to 6.65 GHz, by changing the reverse-biased voltage of the varactor diode from 0.5 V to 10 V. The antenna is $40 \times 40\,\text{mm}^2$ in size and comprises four C-shaped elements.

Recent breakthroughs in laser processing can enhance the planner antenna's performance even further. Laser technology utilizes coherent and high-intensity light to alter the architecture and material characteristics of the antenna. These qualities can lead to better surface roughness, higher conductivity, and improved dielectric properties, all optimizing antenna performance [26]. By accurately adjusting laser properties, it is possible to realize tailored alterations that meet specific design parameters, leading to antennas with wider bandwidths and higher gain [27].

The application of a Neodymium-doped Yttrium Aluminium Garnet (Nd: YAG) laser has been demonstrated to improve both bandwidth and antenna gain [28, 29]. The laser treatment repairs the antenna's physical and microstructural characteristics, achieving significant improvements in electromagnetic performance by modifying its surface and structural characteristics.

This work involves the development and execution of a compact antenna that is reconfigurable and operates at frequencies below 6 GHz. After implementation, the antenna's radiation line undergoes treatment with an Nd: YAG laser to improve its bandwidth and gain. The antenna has a varactor diode that adjusts the frequency range from 4 to 6.65 GHz. This technology enables the advancement of more efficient wireless networks by attaining desirable enhancements in antenna properties. The comparative analysis indicates that the proposed design outperforms previous works regarding compact profile, improved impedance matching, higher efficiency and gain, and broader bandwidth.

This paper comprises the subsequent sections. Section 2 describes the reconfigurable antenna's configuration, and Section 3 presents the proposed antenna's results and discussions of reflection coefficient, laser treatment, and antenna performance in terms of efficiency, gain, and radiation pattern, as well as a comparison with the referenced antennas. Finally, Section 4 presents the conclusion.

2. ANTENNA CONFIGURATION

The top and bottom views of the proposed design, which includes a fabricated prototype of the reconfigurable C-shaped patch antenna, are illustrated in Figs. 1(a)–(d). The proposed system consists of a ground plane that measures $30 \times 20\,\text{mm}^2$ and a C-shaped antenna. The antenna is designed on a Rogers RT5880 substrate with a thickness of 0.8 mm, a relative permittivity of 2.2, and a tangent loss of 0.0009. The impedance of the patch and feed line is matched by a curly stub that is placed adjacent to the radiator's edge, thereby reducing return loss.

The design process is illustrated in Figs. 2(a)–(d), which provides a representation of the sequential steps. A 50-ohm microstrip line provides power to the antenna during the initial stage (step 1). In order to accomplish impedance matching, a stub is implemented in the second step. Nevertheless, issues arise due to the inconsistent impedance of the surface beneath the radiating element, which renders it an ineffective radiator across the interested frequency range. The third step (step 3) is shown in Fig. 2(c), which further advances the process. At this stage, a stub connects an inverted L-shaped parasitic component to the primary element, allowing it to operate in higher frequency bands. This configuration is demonstrated in Fig. 3, which provides a unique perspective on this aspect.

The primary and parasitic L-shaped elements are separated by an etched gap measuring 0.8 mm, which accommodates the varactor diode in further progress. The radiator's continuous function at a resonance of 5 GHz is made possible by the precise configuration, as depicted in Fig. 3, in conjunction with a capacitance of 1.5 pF. The impedance of the patch and feed

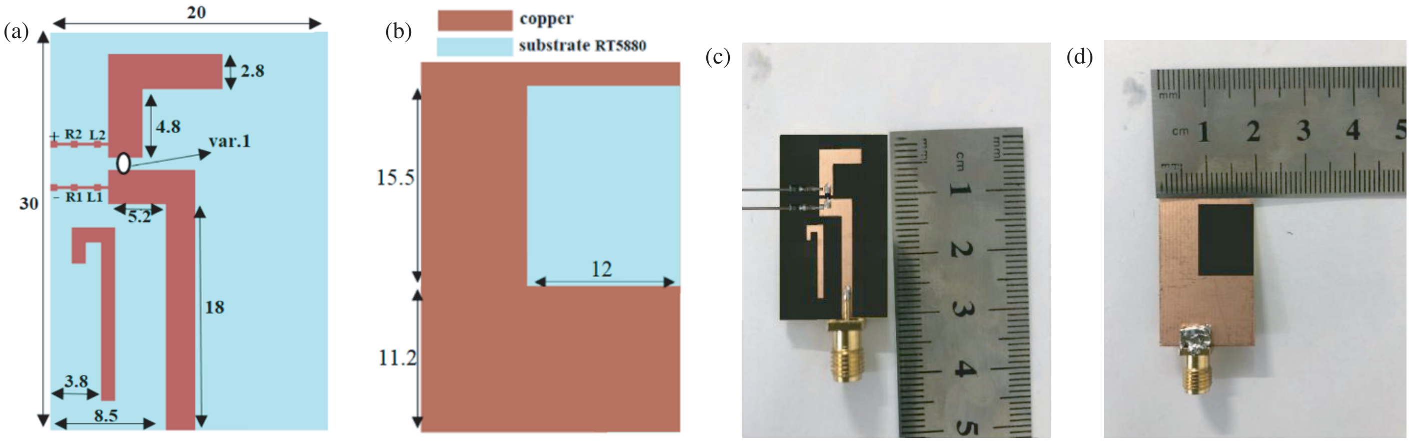

FIGURE 1. Geometry of reconfigurable antenna: (a) Top, (b) Bottom, and (c)–(d) Fabricated prototype view.

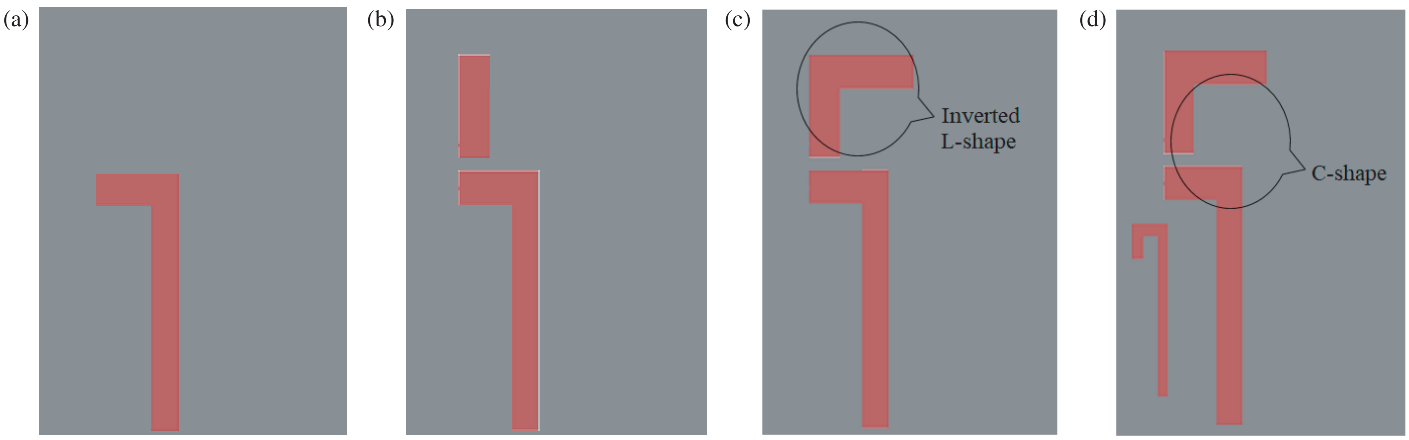

FIGURE 2. Design process of proposed antenna: (a) step 1, (b) step 2, (c) step 3, and (d) step 4.

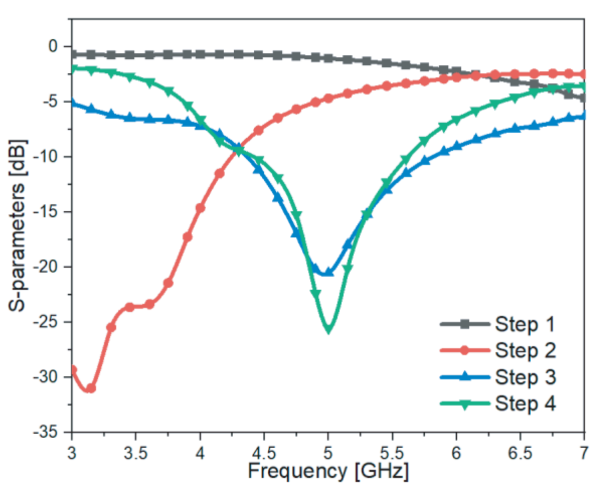

FIGURE 3. Reflection coefficient for the reconfigurable antenna.

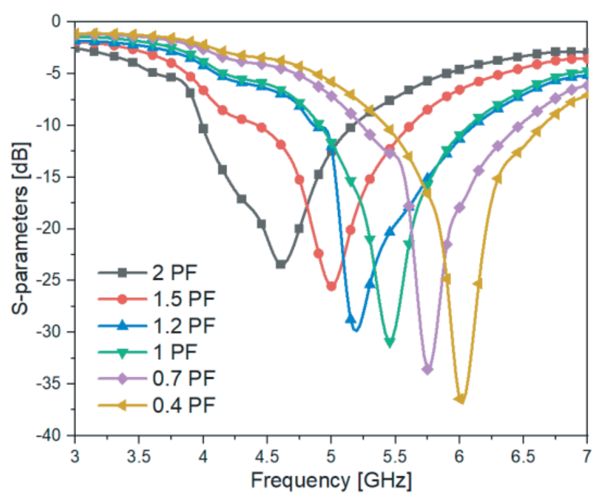

FIGURE 4. Simulated reflection coefficients at six values of capacitance.

line are matched to reduce return loss, which is achieved by positioning a curly patch with size $12 \times 3\,\text{mm}^2$ adjacent to the radiator's edge. This enhancement is illustrated in Fig. 2(d), which denotes the fourth stage of the process.

The physical design of the radiator, essential impedance characteristics, and intended operational frequency range are the critical determinants of the varactor diode's placement. The impedance and resonance frequency of the antenna can be ad-

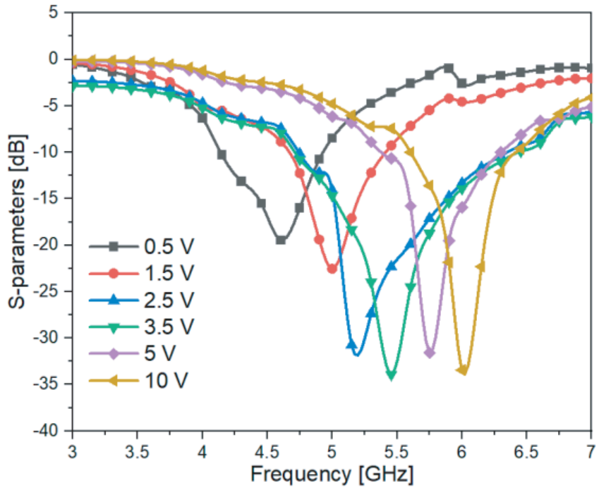

FIGURE 5. Measured reflection coefficients at different voltages.

FIGURE 6. Prototype with ND: YAG laser.

justed by precisely positioning the diode along the radiating element or feed structure. Consequently, this modification has a significant influence on the antenna's effectiveness and bandwidth.

The methodology for determining the fundamental characteristics is explained using the transmission line model [30, 31].

Calculation of the patch width (W) and the effective length (L_{eff}) is illustrated as follows:

$$W = \frac{c}{2f_o}\sqrt{\frac{2}{\varepsilon_r + 1}} \tag{1}$$

$$\varepsilon_{reff} = \frac{\varepsilon_r + 1}{2} + \frac{\varepsilon_r - 1}{2}\left(1 + 12\frac{h}{w}\right)^{-\frac{1}{2}} \tag{2}$$

$$L_{eff} = \frac{c}{2f_o\sqrt{\varepsilon_{reff}}} \tag{3}$$

where f_o indicates the resonance frequency in GHz, c the speed light, ε_r the relative permittivity of the substrate, ε_{reff} the effective dielectric constant, and h the substrate thickness.

The precise patch length (L) is related to length extension (ΔL)

$$\Delta L = \frac{(\varepsilon_{reff} + 0.3)\left(\frac{w}{h} + 0.264\right)}{(\varepsilon_{reff} - 0.258)\left(\frac{w}{h} + 0.8\right)} \tag{4}$$

$$L = L_{eff} - 2\Delta L \tag{5}$$

The antenna's design, shaped like a C, was simulated and improved using a high-performance 3D electromagnetic analysis software called CST.

3. RESULTS AND DISCUSSIONS

3.1. Reflection Coefficient

The simulation and optimization of a reconfigurable antenna design were carried out using a CST Studio Suite. Fig. 4 depicts the evaluation of the reflection coefficient conducted using the CST tool. As described in the datasheet, the frequency tuning experiment entailed modifying the varactor diode's capacitance values within the parameter range of 0.4 to 2 pF.

In order to validate the simulation results achieved from CST, a system prototype was developed. This experimental model is illustrated in Figs. 1(c)–(d). The measurements were carried out using a KC901V model vector network analyzer (VNA) to cover a frequency range from 100 MHz to 7 GHz. The VNA underwent a rapid calibration operation that involved an open/short/load sequence prior to the measurement. A more straightforward approach to measuring the transmission and reflection coefficients has been established: the reverse bias voltage applied to the diode is adjusted from 0.5 to 10 V. The varactor diode SMV2019 is specified to have a minimal bias voltage of 0 V in the datasheet. The outcome is a 0.25 GHz decrease in the resonance frequency.

Figure 5 depicts a comparison measurement of the S-parameter, comparing the simulated and measured values. By increasing the biased voltage of the varactor diode from 0.5 to 10, the lower resonant band was shifted from 4 to 5.18 GHz, while the higher band was shifted from 5.45 to 6.65 GHz.

The voltage standing wave ratio (VSWR) and characteristic impedance are two important factors that define the characteristics of the design that are being suggested.

One way to measure the efficiency of transmitting radio-frequency power from a power source to a load is by looking at the VSWR. To test impedance matching in radio-frequency systems, one uses the maximum-to-minimum amplitude ratio of the standing wave. A VSWR of $1 : 1$ indicates perfect alignment with little reflection and power loss. The inherent impedance of a transmission line, often 50 ohms in RF applications, is known as the characteristic impedance. It shows a single wave's relationship with its voltage and current. With VSWR and impedance values below 1.5 and about 49 ohms, the reconfigurable antenna is effectively transmitting power and has good impedance matching.

3.2. Particle and Roughness Analysis

The analysis of the nanoparticles shows that the surface is generally clean and even with limited particulate matter before us-

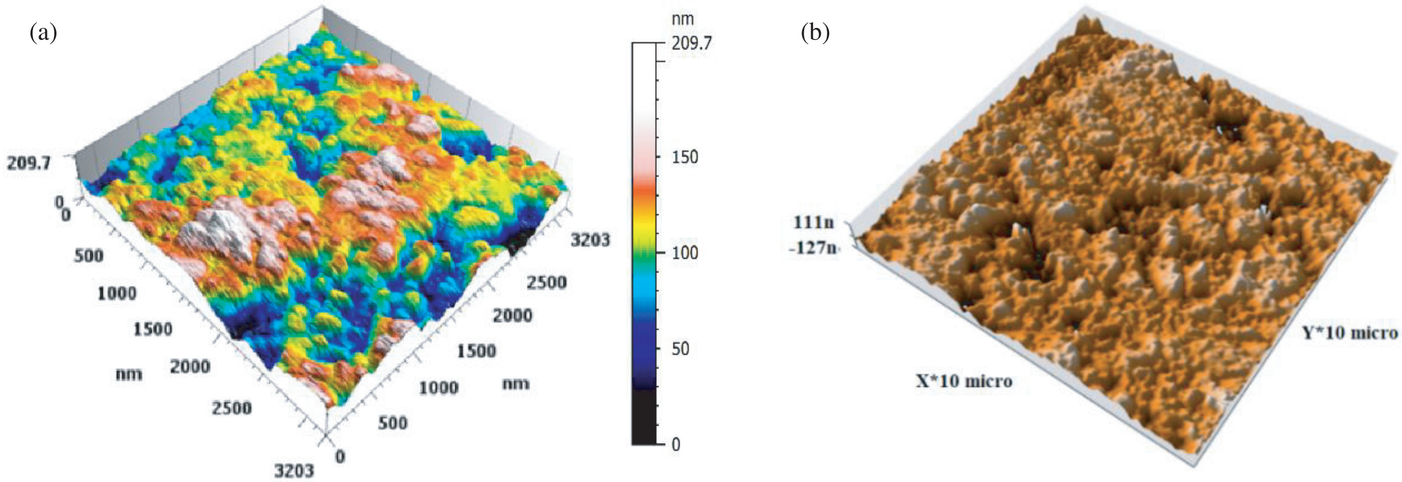

FIGURE 7. Particle and roughness before laser treatment. (a) Particle analysis. (b) Surface roughness.

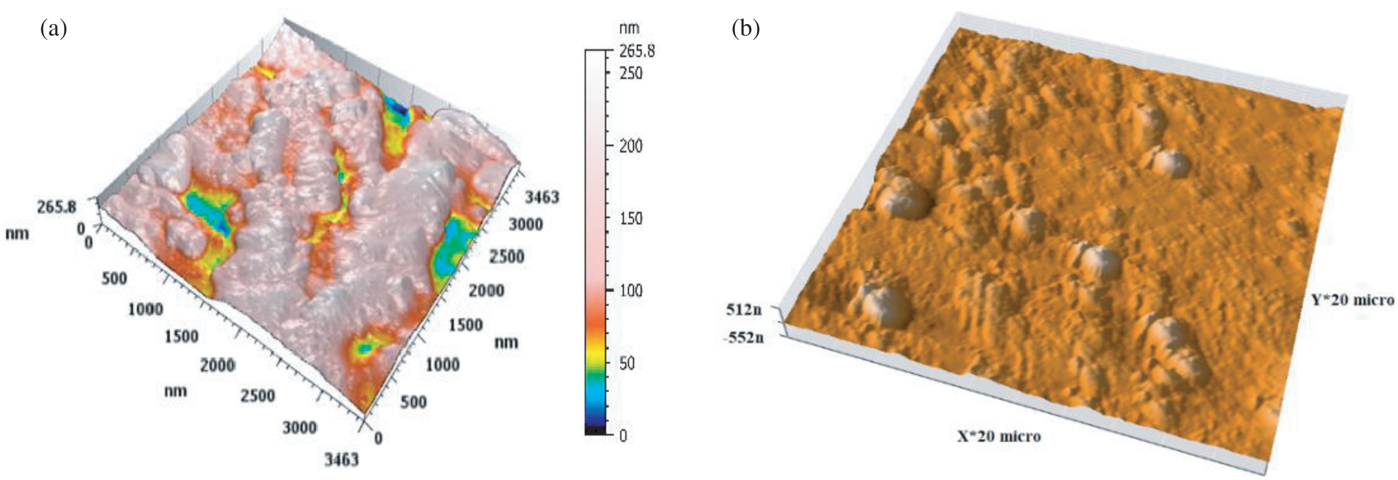

FIGURE 8. Particle and roughness After laser treatment. (a) Particle analysis. (b) Surface roughness.

ing the ND: YAG laser on the structure of the reconfigurable C-shaped patch antenna mounted on a Rogers RT dielectric substrate (Fig. 6). The particles that are present are frequently exceedingly small, typically falling within the micron to sub-micron range, as illustrated in Fig. 7(a). Atomic force microscopy (AFM) was used to measure the standard roughness, as shown in Fig. 7(b). Surface roughness metrics are found to be low in the results.

Significant modifications to the surface make it quite rough. As observed in Fig. 8(a), this appearance is the result of the material's melting, vaporization, and re-solidification processes. As vaporized material condenses into debris particles of varying sizes, the surface encounters non-uniformity in particle size and distribution.

According to roughness examination, surface roughness metrics, like Ra and Rq, show a notable increase following laser application. Fig. 8(b) shows that as a result, the surface becomes increasingly uneven, with more pronounced peaks and valleys and overall undulation. The increased roughness affects the material's conductive layers and dielectric properties, changing the surface structure.

To illustrate the variation, Fig. 9 presents a comparison of the measured scattering parameters for the designed antenna, both with and without treatment. With no modifications, the antenna covers a wide frequency range of 4.5 to 5.5 GHz, and its 5 GHz resonance frequency is achieved with a biasing voltage of 1.5 V. The antenna's ND: YAG laser covers a wide frequency range of 4.45 to 5.6 GHz. As shown in Fig. 9, it displays resonances at 5 GHz. There is a significant correlation between the pre- and post-treatment simulated and measured outcomes of the proposed configuration.

3.3. Performance of the Proposed Design

A comprehensive analysis has been performed on the antenna's gain and total efficiency parameters in different states, as shown in Fig. 10. Specified frequency ranges in which the antenna operates include 4.25–6.48 GHz, 5.18–5.18 GHz, 5.25–5.5 GHz, 5–6 GHz, and 5.45–6.65 GHz. Within the specified frequency ranges, the minimum gain recorded is 3.8 dBi, with an efficiency of 90%. In contrast, the antenna attains a maximum gain of 4.3 dBi and a peak overall efficiency of 94%. An impor-

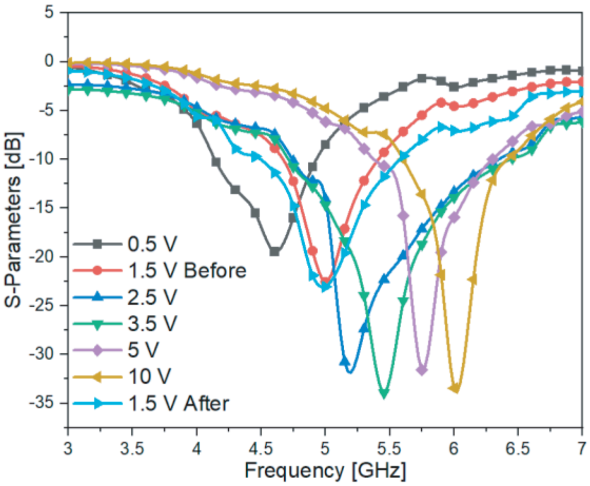

FIGURE 9. Measured reflection coefficients before and after treatment at 1.5 V (5 GHz).

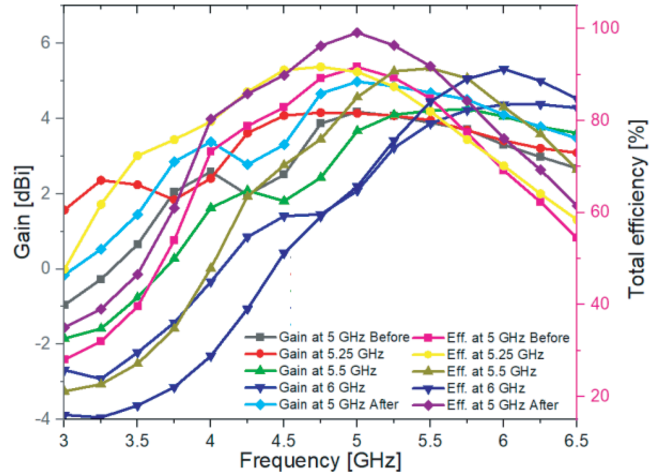

FIGURE 10. Evaluation of the proposed design's gain and efficiency.

TABLE 1. Comparison with previous works.

Ref. No.	Antenna size (mm^2)	No. of Diodes	Frequency (GHz)	Bandwidth (GHz)	Gain (dBi)	Eff. (%)
[16]	45 × 89	2	2.4	2.15–2.63	10	88
[17]	36 × 48	4	2 and 2.4	1.88–2.64	4	82
[18]	35 × 47.25	2	2.4, 3.6, 5.1	2.2–2.8, 3.4–3.8, 4.8–6	4.2	78
[19]	37 × 72	2	1.8	1.7–1.9	6.28	N.M
[20]	15 × 25	2	3.7 and 6.2	3.3–4.2, 5.8–7.2	3.4	92
[21]	150 × 150	4	2.04, 2.5, 2.98	1.5-3.5	4.91	62
[22]	50.5 × 41.5	3	2.2, 2.4, 2.5, 2.7	1.91–2.77	1.57	N.M
[23]	31 × 42.04	2	3.1, 3.6, 3.8	3–4	2.27	95
[24]	60 × 70	1	2.07, 4.63, 6.22	1.8–2.3, 4.3–4.8, 6–6.4	5.68	74
This work	20 × 30	1	4.5, 5, 5.25, 5.5, 5.75, 6	4–5.1, (4.5–5.5 Before) (4.45–5.6 After), 5–6, 5.2–6.4, 5.4–6.6	(4.3 Before) and (5 After)	90 95

tant observation is that the gain of the reconfigurable modified monopole C-shaped antenna rises as the frequency increases.

A more thorough examination of the antenna's performance, both with and without modification, shows that the gain continuously exceeds 3.8 dBi throughout its frequency range. More precisely, by operating at a resonance frequency of 5 GHz, the antenna achieves a maximum gain of 4.3 dBi. The treatment application increases the antenna's gain by around 15%, leading to a maximum gain of 5 dB compared to the previous state. The measurable gain strongly corresponds to the predicted outcomes, confirming the findings' dependability.

Moreover, the antenna under consideration has a radiation efficiency approaching 90% within its designated operational range. At the resonance frequency of 5 GHz, the laser-loaded antenna attains a maximum radiation efficiency of 97.5% at a frequency of 5 GHz, validating the proposed treatment's effectiveness in improving both the gain and efficiency.

Figure 11 shows the E- and H-plane two-dimensional radiation patterns at four frequencies (5, 5.25, 5.5, and 6 GHz). A review of the results shows that the E-plane properties at higher frequencies are similar to those at lower frequencies. At each of the four frequencies used in the experiment, the co-polarizations in the E-plane exceed the H-plane cross-polarizations. However, co- and cross-polarization discrepancies point to an advantageous E-plane radiation pattern. Also, the cross-polarization is smaller, and the E-plane co-polarizations behave almost quasi-omnidirectional. The substantial deviation leads to a steady radiation pattern in the E-plane.

3.4. Comparison with Previous Research Articles

Table 1 summarizes the performance evaluation of the proposed antenna design compared to previous works. The results show that the recommended configuration is effective for various critical parameters. In particular, the proposed antenna exhibits a frequency range of 1.1 GHz, significantly wider than the

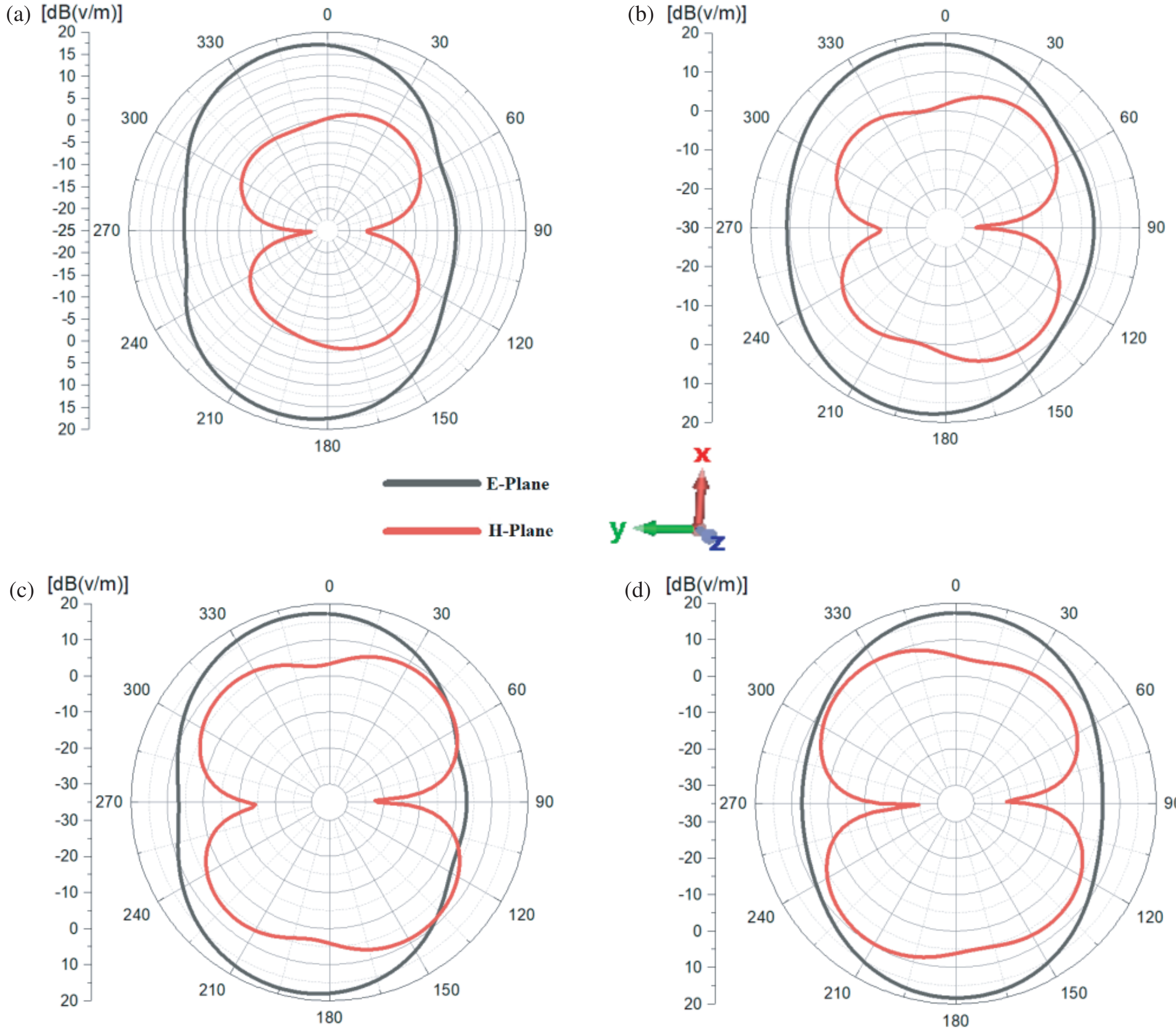

FIGURE 11. 2-D electric field radiation pattern at four frequencies: (a) 5 GHz, (b) 5.25 GHz, (c) 5.5 GHz, and (d) 6 GHz.

reference designs. Additionally, the design outperforms the efficiency of numerous existing configurations by 97%.

The proposed antenna's gain, which is five dBi, is comparable to that of the referenced designs. In addition, the proposed design's impedance matching is nearly optimal, with a value of approximately 50 Ohms, ensuring efficient power transfer and minimal signal loss. This is further confirmed by the VSWR value of approximately one, which suggests a transmission line that is nearly perfect and minimally reflected waves.

The suggested antenna is physically compact, with $20 \times 30\,\text{mm}^2$ dimensions. This antenna is advantageous for modern communication devices requiring a compact form factor. It is both efficient and compact. The proposed antenna is distinguished from other published designs by including a ground clearance zone area expressly designed for the sub-6 GHz frequency bands. This optimization improves the antenna's overall performance by increasing the total efficiency across a wide range of frequency bands and spanning a broad bandwidth.

4. CONCLUSION

This paper presents a compact, reconfigurable C-shaped patch antenna designed for 5G applications within the sub-6 GHz spectrum. Integrating Nd: YAG laser treatment and a varactor diode for frequency tuning has led to significant enhancements in bandwidth and gain, achieving a bandwidth of 1100 MHz and a gain of 5.2 dBi at 5 GHz. The antenna's compact size ($20 \times 30\,\text{mm}^2$) and efficient operation across multiple frequencies make it well suited for modern wireless communication devices. Compared to existing designs, the proposed antenna demonstrates high performance, particularly in broader bandwidth, improved gain, and nearly ideal impedance matching, with a reflection coefficient consistently below -10 dB. The matching between the simulated and measured results confirms the design's effectiveness and highlights its potential for sub-6 GHz applications.

ACKNOWLEDGEMENT

The authors are grateful for the assistance of Al-Iraqia University (https://en.aliraqia.edu.iq/) in developing this work.

REFERENCES

[1] Balanis, C. A., *Antenna Theory: Analysis and Design*, John Wiley & Sons, 2016.

[2] Song, X., T.-L. Zhang, and Z.-H. Yan, "Broadband and low-profile slot antenna with AMC surface for X/Ku applications," *Progress In Electromagnetics Research M*, Vol. 71, 189–197, 2018.

[3] Kareem, Q. H., R. A. Shihab, and H. H. Kareem, "Compact dual-polarized reconfigurable MIMO antenna based on a varactor diode for 5G mobile terminal applications," *Progress In Electromagnetics Research C*, Vol. 137, 185–198, 2023.

[4] Ma, R., Y. Gao, Y. Wang, and C. Parini, "Circular co-planar inverted-F antenna for UHF machine-to-machine communications," in *2015 IEEE International Symposium on Antennas and Propagation & USNC/URSI National Radio Science Meeting*, 1418–1419, Vancouver, BC, Canada, Jul. 2015.

[5] Prabhakar, D., P. M. Rao, and M. Satyanarayana, "Characteristics of patch antenna with notch gap variations for Wi-Fi applications," *International Journal of Applied Engineering Research*, Vol. 11, No. 8, 5741–5746, 2016.

[6] Rahayu, Y. and M. I. Hidayat, "Design of 28/38 GHz dual-band triangular-shaped slot microstrip antenna array for 5G applications," in *2018 2nd International Conference on Telematics and Future Generation Networks (TAFGEN)*, 93–97, Kuching, Malaysia, Jul. 2018.

[7] Srivastava, K., B. Mishra, A. K. Patel, and R. Singh, "Circularly polarized defected ground stub-matched triple-band microstrip antenna for C- and X-band applications," *Microwave and Optical Technology Letters*, Vol. 62, No. 10, 3301–3309, 2020.

[8] Hossain, A., M. T. Islam, M. E. H. Chowdhury, and M. Samsuzzaman, "A grounded coplanar waveguide-based slotted inverted delta-shaped wideband antenna for microwave head imaging," *IEEE Access*, Vol. 8, 185 698–185 724, 2020.

[9] Boontamchauy, P., T. Lertwiriyaprapa, and C. Phongcharoenpanich, "Inverted L-shaped CP patch antenna with corner-truncated partial ground plane diagonally adjoined with square branch for L-band applications," *Sensors*, Vol. 21, No. 4, 1085, 2021.

[10] Priyalatha, P., R. Kumari, and S. Nandi, "Compact modified hourglass-shaped aperture-coupled antenna for radar applications," *International Journal of Microwave and Wireless Technologies*, Vol. 15, No. 9, 1592–1600, 2023.

[11] Kumar, K. P., K. S. Rao, V. M. Rao, K. Uma, A. Somasekhar, and C. M. Mohan, "The effect of dielectric permittivity on radiation characteristics of co-axially feed rectangular patch antenna: Design & analysis," *International Journal of Advanced Research in Computer and Communication Engineering*, Vol. 2, No. 2, 1254–1258, 2013.

[12] Kim, J.-H. and B.-G. Kim, "Effect of feed substrate thickness on the bandwidth and radiation characteristics of an aperture-coupled microstrip antenna with a high permittivity feed substrate," *Journal of Electromagnetic Engineering and Science*, Vol. 18, No. 2, 101–107, 2018.

[13] Kedze, K. E., H. Wang, Y. B. Park, and I. Park, "Substrate dielectric constant effects on the performances of a metasurface-based circularly polarized microstrip patch antenna," *International Journal of Antennas and Propagation*, Vol. 2022, No. 1, 3026677, 2022.

[14] Hussain, R., A. Raza, M. U. Khan, A. Shammim, and M. S. Sharawi, "Miniaturized frequency reconfigurable pentagonal MIMO slot antenna for interweave CR applications," *International Journal of RF and Microwave Computer-Aided Engineering*, Vol. 29, No. 9, e21811, 2019.

[15] Kareem, Q. H. and M. J. Farhan, "Compact dual-polarized eight-element antenna with high isolation for 5G mobile terminal applications," *International Journal of Intelligent Engineering and Systems*, Vol. 14, No. 6, 187–197, 2021.

[16] Kovitz, J. M., H. Rajagopalan, and Y. Rahmat-Samii, "Design and implementation of broadband MEMS RHCP/LHCP reconfigurable arrays using rotated E-shaped patch elements," *IEEE Transactions on Antennas and Propagation*, Vol. 63, No. 6, 2497–2507, 2015.

[17] Alam, M. S. and A. M. Abbosh, "Wideband pattern-reconfigurable antenna using pair of radial radiators on truncated ground with switchable director and reflector," *IEEE Antennas and Wireless Propagation Letters*, Vol. 16, 24–28, 2016.

[18] Chattha, H. T., N. Aftab, M. Akram, N. Sheriff, Y. Huang, and Q. H. Abbasi, "Frequency reconfigurable patch antenna with bias tee for wireless LAN applications," *IET Microwaves, Antennas & Propagation*, Vol. 12, No. 14, 2248–2254, 2018.

[19] Abdulkawi, W. M., A.-F. A. Sheta, W. A. Malik, S. U. Rehman, and M. S. Alkanhal, "RF MEMS switches enabled H-shaped beam reconfigurable antenna," *The Applied Computational Electromagnetics Society Journal (ACES)*, Vol. 34, No. 9, 1312–1319, 2019.

[20] Awan, W. A., S. I. Naqvi, W. A. E. Ali, N. Hussain, A. Iqbal, H. H. Tran, M. Alibakhshikenari, and E. Limiti, "Design and realization of a frequency reconfigurable antenna with wide, dual, and single-band operations for compact sized wireless applications," *Electronics*, Vol. 10, No. 11, 1321, 2021.

[21] Muthuvel, S. K. and Y. K. Choukiker, "Wideband frequency agile and polarization reconfigurable antenna for wireless applications," *IETE Journal of Research*, Vol. 69, No. 3, 1529–1538, 2023.

[22] Hossain, K., T. Sabapathy, M. Jusoh, P. J. Soh, R. B. Ahmad, M. I. Jais, M. N. Osman, M. N. M. Yasin, H. A. Rahim, N. Saluja, and Q. H. Abbasi, "A frequency-reconfigurable microstrip antenna with constant dipole-like radiation patterns using single bias, triple varactor tuning with reduced complexity," *Wireless Personal Communications*, Vol. 123, 1003–1024, 2022.

[23] Lavadiya, S. P., V. Sorathiya, S. Kanzariya, B. Chavda, A. Naweed, O. S. Faragallah, M. M. A. Eid, and A. N. Z. Rashed, "Low profile multiband microstrip patch antenna with frequency reconfigurable feature using PIN diode for S, C, X, and Ku band applications," *International Journal of Communication Systems*, Vol. 35, No. 9, e5141, 2022.

[24] Sakkas, A., V. Oikonomou, G. Mystridis, V. Christofilakis, G. Tatsis, G. Baldoumas, V. Tritiakis, and S. K. Chronopoulos, "A frequency-selective reconfigurable antenna for wireless applications in the S and C bands," *Sensors*, Vol. 23, No. 21, 8912, 2023.

[25] Al-Gertany, Q. H. K. and Q. Hadi, "Reconfigurable compact wide-band quad-port antennas based on a varactor diode for sub-6 GHz 5G communications," *Progress In Electromagnetics Research C*, Vol. 145, 91–100, 2024.

[26] Ghanim, A. M., M. Hussein, M. F. O. Hameed, A. Yahia, and S. S. A. Obayya, "Highly directive hybrid Yagi-Uda nanoantenna for radition emission enhancement," *IEEE Photonics Journal*, Vol. 8, No. 5, 1–12, 2016.

[27] Hayashi, J., C. Liu, F. Akamatsu, A. Nishiyama, A. Moon, and Y. Ikeda, "Effects of microwave-enhanced plasma on laser ignition," in *Ignition Systems For Gasoline Engines: 3rd International Conference, Germany*, 245–253, Nov. 2017.

[28] Kausas, A. and T. Taira, "Giant-pulse Nd:YVO4 microchip laser with MW-level peak power by emission cross-sectional control," *Optics Express*, Vol. 24, No. 4, 3137–3149, 2016.

[29] Saiki, T. and A. Tatebayashi, "Microchip Nd: YAG and Nd: YVO4 lasers pumped by VHG wavelength-stabilized laser diode," *International Journal of Optics*, Vol. 2020, No. 1, 3952435, 2020.

[30] Abdullah, L. W., Q. H. Kareem, and A. H. Sallomi, "A quad-port multiple-input-multiple-output system for underlay or interweave cognitive radio," *Indonesian Journal of Electrical Engineering and Computer Science*, Vol. 29, No. 3, 1480–1495, 2023.

[31] Mohamed, A. J., H. F. Khazaal, T. H. Abed, and Q. H. Kareem, "Design and implementation of a multi-band quad-port MIMO antenna for the 5G applications," in *2023 Second International Conference on Advanced Computer Applications (ACA)*, 1–6, Misan, Iraq, Feb. 2023.